Environmental Science Advances

ROYAL SOCIETY OF CHEMISTRY

PAPER

View Article Online
View Journal | View Issue

Cite this: *Environ. Sci.: Adv.*, 2023, **2**, 1727

Physicochemical and microbiological effects of geological biomethane storage in deep aquifers: introduction of O_2 as a cocontaminant†

P. G. Haddad,[a] M. Ranchou-Peyruse, [abc] M. Guignard,[c] J. Mura, [a] F. Castéran,[ab] P. Sénéchal,[d] M. Larregieu,[c] M.-P. Isaure, [c] P. Moonen,[d] I. Le Hécho, [bc] G. Hoareau,[e] P. Chiquet,[bf] G. Caumette,[bf] A. Petit,[g] P. Cezac[ab] and A. Ranchou-Peyruse [*bc]

Biomethane is considered one of the most promising energy vectors to substitute fossil fuels during the global energy transition. Its production is steadily increasing, and high storage volumes are needed to cover seasonal needs. Existing underground gas storage (UGS) aquifers, which have been used for natural gas storage, are excellent candidates. Underground aquifers are known for being anoxic systems. However, dioxygen (O_2) can be injected as an impurity with biomethane into these anoxic environments. O_2 limitations in the underground vary worldwide; however projects are conducted to optimize these limitations. It has been shown that O_2 presence can affect the aquifer's ecosystems and induce mineral reactions. Thus, a multidisciplinary study was conducted in which the *in situ* conditions were simulated in a high-pressure reactor. Water containing autochthonous microorganisms and reservoir rock were used as the aqueous and solid phases, respectively. Initially, the gas phase was composed of methane, 1% CO_2, benzene and toluene under 60 bar and 36 °C conditions. Sulfate was depleted from the aqueous phase due to sulfate-reducing microorganismes. After 50 days, 100 ppm O_2 was injected into the gas phase. Sulfate reducers were inactivated; however, other taxonomic groups became dominant, such as members of the class Acidobacteriae and the families *Desulfitobacteriaceae* and *Kineosporiaceae*. Hydrocarbon biodegradation was demonstrated by a benzene decrease in the aqueous phase, which was barely affected by O_2 injection. However microbial analyses suggested a shift in the ecosystem to adapt to this new 'low aerobic' conditions. The findings of this study can help for better understanding of any other process including O_2 as an impurity in UGS such as CCS and CAES.

Received 13th April 2023
Accepted 25th October 2023

DOI: 10.1039/d3va00086a

rsc.li/esadvances

Environmental significance

With the biomethane sector development, there is an increase of its injection in the natural gas network, including geological storages. Before its injection, O_2 is added to eliminate sulfides. A co-injection of O_2 is expected in geological storage (accepted limit of 100 ppm), such as deep aquifers, which host autochthonous microorganisms. This O_2 threatens strictly anaerobic microorganisms and their biodegradation activities of monoaromatic hydrocarbons coming from the gas storage. Multidisciplinary studies mimicking deep aquifer conditions are essential to confirm or adapt the authorized limits of O_2. Our study showed no major modification of aquifer rocks (minerals and porosity) but a shift of the diversity of the community, eliminating the less resistant ones and creating a new equilibrium allowing benzene degradation.

Introduction

Biomethane may provide a new, reliable and sustainable source of energy and an effective alternative to fossil fuels. After carbon dioxide (CO_2), hydrogen sulphide (H_2S) and water removal, biogas is essentially composed of biomethane. Biomethane is gaining interest and governments are encouraging methanization units. In France, for example, the aim is to increase the share of renewable gas in the gas network to up to 10% by 2030.[1] Concurrently, Europe launched the REPowerEU project that aims to speed up the roll-out of renewable gases. One of the

[a]*Universite de Pau et Pays de l'Adour, E2S UPPA, LaTEP, Pau, France*
[b]*Joint Laboratory SEnGA, UPPA-E2S-Teréga, 64000, Pau, France*
[c]*Universite de Pau et Pays de l'Adour, E2S UPPA, CNRS, IPREM, Pau, France. E-mail: anthony.ranchou-peyruse@univ-pau.fr; Tel: +33 540 145 164*
[d]*Universite de Pau et Pays de l'Adour, E2S UPPA, CNRS, DMEX, Pau, France*
[e]*Universite de Pau et Pays de l'Adour, E2S UPPA, CNRS, TotalEnergies, LFCR, Pau, France*
[f]*Teréga, Pau, France*
[g]*STORENGY – Geosciences Department, Bois-Colombes, France*

† Electronic supplementary information (ESI) available. See DOI: https://doi.org/10.1039/d3va00086a

objectives was to attain a biomethane production of 35 billion cubic metres per year by 2030, while its production was at 3.6 billion cubic metres by the end of 2021.[2] To optimize biomethane use as a major energy source, gas storage facilities of sufficient volumes must be made available. The use of existing underground geological storage (UGS) sites that are known for their large capacities is important, especially to store large volumes to supply during periods of high gas demand, energy crises or even in the case of political issues. Moreover, the use of UGS seems rational since it is beneficial to use the existing infrastructure and network.

Among UGS solutions, deep aquifers are known for their capacity to store large volumes of gas under pressure under anoxic conditions and to be home of anaerobic microbial communities.[3,4] Sulfate-reducing microorganisms (SRMs) were the most frequently detected microorganisms in deep aquifers.[4–12] Sulfate quantities in UGS aquifers have been observed to decrease at multiple sites.[4] Nevertheless, an important product of SRMs is H_2S, which can lead to UGS problems such as corrosion of wells and souring.[13] However, studies have also shown the capability of SRMs to degrade monoaromatic hydrocarbons found in natural gas storage mixes, especially benzene, toluene, ethylbenzene and xylene (BTEX).[6,9,12,14,15]

One of the main differences between natural gas and biomethane is the potential presence of oxygen (O_2) in the latter.[16] In fact, O_2 is used to remove the undesirable H_2S compounds present in the biomethane product. The current European recommendations are that the O_2 content must not exceed 100 ppm within the gas circulating in the network and possibly in UGS.[17–19] In UGS, O_2 can also be present as an impurity during CO_2 capture and storage (CCS)[13,18,20–22] and in compressed air for energy storage (CAES).[23–25] O_2 can also be intentionally injected for enhancing oil recovery[26–28] and for the bioremediation of groundwater.[29,30] O_2 that is injected into deep aquifers not only affects microbial life but also interacts with mineral phases.[25] One example is mineral oxidation, which depends on the nature of the solid phase.[9,22,31–33] Recently, a study with 1% O_2 was carried out since it corresponds to the maximum quantity found in biomethane.[9,16] The results indicated the deleterious effect of O_2 on microbial life. Bioattenuation of monoaromatic hydrocarbons ceased.

Here, the experiment was performed to understand the effect of 100 ppm (0.01%) O_2, the maximum quantity authorized to circulate in the gas grid today. The conditions of an UGS aquifer were reproduced in a high-pressure (HP) reactor for 86 days and the results provided evidence for the potential impact of O_2 introduction based on the current recommended limits. This multidisciplinary study permitted to understand the effect of O_2 on the physicochemical parameters of the storage, on the microbial ecosystem developed underground and on the minerals found in the reservoir rock. The experimental work consisting of reproducing the aquifer used as UGS in a HP reactor with its different phases (gas, solid and liquid with autochthonous microorganisms) allowed observing the effects of 100 ppm O_2 under the *in situ* conditions, the maximum concentration recommended in Europe. Indeed, this concentration limit of O_2 was established based on gas transport optimization, and storage conditions were not considered. Thus, studies are still needed to reconsider O_2 limits in injected biomethane to protect UGS reservoirs. This work is the first to evaluate the effects of this O_2 concentration limit on UGS in a deep aquifer.

Materials and methods

Site description, formation water and reservoir rock characteristics

The UGS aquifer is situated in the Aquitaine sedimentary basin (582 m depth) in southwestern France.[9] The selected monitoring well, denoted as Ab_L_1, is closest to the UGS.[4] The formation water was obtained more than a year before the experiment due to COVID restrictions. The samples were stored in anaerobic bottles at 4 °C. The main anions comprising the formation water were chloride (0.35 mM) and sulfate (0.02 mM) (Table S1†). Two underground samplings were performed to recover 0.578 L and 0.556 L of water containing autochthonous microorganisms. Samplings were carried out from the site using two downhole samplers equipped with a PDS Sampler (Leutert Bottom Hole Positive Displacement Sampler[33]). Formation water was also sampled from the wellhead and was filter-sterilized (PES 47 mm membranes, 0.1 μm, Sartorius) under anoxic conditions and stored at 4 °C before use. A volume of 0.591 L of the filtered wellhead water was added to both volumes of the recovered formation water to yield the aqueous phase that was injected into the HP reactor. A volume of 0.1 L was taken from the final mixture for microbial diversity study (day 0), and the remaining (1.39 L) was injected into the reactor. On day 39 of the experiment, formation water supplemented with sulfate (0.60 mM) was added to maintain the system. The reservoir rock consisted of inframolassic sands.[4,9] Cuttings were collected from a drilling carried out near the studied site.

Experimental apparatus and analysis techniques

The entire experimental protocol has been schematically summarized in the form of a flowchart (Fig. S1†).

High-pressure (HP) reactor. The experimental apparatus consisted of a HP reactor as previously described.[9,10] Briefly, the reactor was made of Hastelloy C-276 to avoid corrosion problems. The autoclave was heated by using heating resistors with insulating coatings. To maintain the temperature of the apparatus, a double jacket was installed. The temperature was monitored by using thermocouples in both gas and aqueous phases. Both phases were mixed using a double disc stirrer with four vertical blades for the gas one and a Rushton turbine for the aqueous one, with a stirring speed of 20 rpm. The solid phase was in a basket, which was made of Teflon. Its bottom was composed of a Hastelloy C-276 disc with 10 μm pores to prevent mineral particles from falling out.

Physicochemical analyses. Ion chromatography (Dionex Integrion HPIC; Thermo Fisher Scientific) was used to quantify fluoride, acetate, chloride, and sulfate ions. Water samples from the reactor were collected and immediately analysed for

the redox potential Eh (Mettler Toledo International Inc.). The gas phase was monitored throughout the experiment using in-line gas chromatography with a microthermal conductivity detector (GC-μTCD; Micro GC Fusion; Chemlys). Using this technique, CH_4, CO_2, O_2, H_2 and N_2 were quantified in the gas phase. The aqueous and gaseous phase compositions were detected with a measurement uncertainty of 5%. More detailed specifications were presented previously.[9] The gas quantities were calculated based on the total pressure measured by using a barometer and the gas phase composition was analysed by gas chromatography according to the real gas law corrected by the compressibility factor estimated by PhreeqC (2.4). The Eh of the aqueous phase collected from the reactor under strict anoxic conditions was monitored weekly at atmospheric pressure (Mettler-Toledo™ SevenCompact™).

Benzene and toluene were quantified in the aqueous and gaseous phases throughout the experiment using a Thermo Fisher Scientific gas chromatograph coupled with a quadrupole mass spectrometer (GC-MS) (ISQ QD Single Quadrupole MS – Trace 1310), in agreement with the specifications detailed previously.[9]

X-ray tomography and mineralogical analyses. Three capillaries made of borosilicate with an internal diameter of 2 mm and a height of 3 cm were filled with the solid phase and placed in the Teflon basket. The top, middle and bottom of each capillary were scanned by X-ray tomography before and after the experiment. A comparison of both enabled the detection of morphological alterations in the solid phase and the presence of microorganisms in the water phase or on the surface of the solid grains. The initial scans were performed in a dry state. For the final scans performed at the end of the experiment, the capillaries were sealed with waterproof glue at room temperature in an anaerobic glove box. A Zeiss Xradia Versa 510 X-ray tomograph was utilized for the scans, and a voxel size of 2.5 microns and a square field of view of 2.5 × 2.5 mm^2 were employed.[9,10]

The remaining solid phase was analysed by X-ray diffraction (XRD) before and after the experiment to detect any variations in the mineral phase. Samples were collected from the basket at four different depths at room temperature in an anaerobic glove box. The samples were then dried with N_2 gas flux to limit mineral oxidation, manually ground and sieved (<100 μm) into a homogeneous powder. The solid powders were then mounted on holders and directly analysed by XRD. The analyses were performed using a Bruker D2 Phaser powder diffractometer equipped with a Cu Kα radiation source. The XRD patterns were recorded over a 5° to 90° 2Θ range with a 0.02° step and a 0.5 s counting time per step. DIFFRAC.EVA software was used to identify the mineral phases.

Aliquots of the same samples collected at four different depths from the basket were submitted for a petrographic study using scanning electron microscopy coupled to energy dispersive spectroscopy (SEM-EDS). Solid pieces were directly mounted on PIN stubs and coated with carbon. Observations and mineral identification were performed with a JEOL JSM 7800F Prime SEM-FEG equipped with an Oxford Instruments AZtecEnergy EDS SDD X-Max 80 mm^2 detector at the Castaing Center in Toulouse, France.

Microbial analyses

Nucleic acid extraction and RNA reverse transcription. Samples from the aqueous phase were collected throughout the experiment with the aim of coextracting nucleic acids (DNA and RNA). Aqueous samples were collected from the reactor and directly filtered using 47 mm PES membrane filters of 0.1 μm porosity (Sartorius Stedim). The filters containing the samples were then stored at −80 °C. Subsequently, the filters were crushed in liquid nitrogen, and the nucleic acids were collected using a Fast RNA Prosoil Direct kit (MP BIO). Then, DNA and RNA were separated using AllPrep RNA/DNA (Qiagen). The extracted DNA and RNA were quantified using a Quant-it™ dsDNA HS (Invitrogen) kit and a Quant-it™ RiboGreen (Invitrogen) kit, respectively. To measure the extracted DNA and RNA, a BioTEK SYNERGY HTX microplate reader was used. The reverse transcriptase M-MLV (Invitrogen™) was used to achieve reverse transcription of the RNA.

Polymerase chain reaction and sequencing. To study global microbial diversity, the V4–V5 region of *16S rRNA* genes and complementary 16S rDNA were amplified by PCR (2700 Thermal Cycler, Applied Biosystems). To reduce the deleterious effects of PCR inhibitors, 1 mg mL^{-1} of BSA (Bovine Serum Albumin, NEB-B9200S) was added to the reagent mix (Taq PCR Core Kit, Roche). For sequencing, the PCR primer set (515F-928R[34]) contained the adapters GTGYCAGCMGCCGCGGTA (forwards) and CCCCGY-CAATTCMTTTRAGT (reverse). Sequencing was performed by using the GenoToul genomic platform (Toulouse, France) using Illumina MiSeq 2 × 250 bp technology. The resulting sequencing data represented 511 618 reads. Raw sequences were archived in the public NCBI database (BioProject ID PRJNA930342). These data were analysed *via* the FROGS pipeline (GenoToul genomics platform in the Galaxy interface).[35] Preprocessing resulted in 424 552 reads that were clustered into OTUs taxonomically classified with the Silva database (release 138.1) and into groups at the taxonomic family level to monitor the evolution of taxonomic diversity during the experiment.

Quantitative PCR. Genes and transcripts of the *16S rRNA*, *dsrB* and *mcrA* genes were quantified to monitor the activity of the overall microbial community, SRM and methanogenic archaea separately at different times during the experiment in the HP reactor. Quantitative PCR was performed with a Takyon NO ROX SYBR 2X MasterMix blue dTTP kit (Eurogentec) according to the supplier's instructions and with a Bio-Rad CFX Connect. The primer pairs consisted of 515F-928R34 (400 nM), DSR 2060F-DSR 4R[36,37] (300 nM), and mlas–mcrArev[38,39] (400 nM). The number of copies of transcripts was calculated using a standard with serially 10-fold diluted pCR™ 2.1-TOPO plasmid (TOPO TA cloning kit, Invitrogen).

Experimental protocol

Before reservoir rock samples were introduced into the HP reactor, they were rinsed with isopropanol and demineralized water to eliminate potential hydrocarbons and drilling brine salts. The solid phase was then dried overnight at 90 °C. Once the solid phase was ready, capillaries were filled with solid samples and were analysed *via* X-ray tomography before the

experiment.[9] Filled and scanned capillaries were placed in a basket containing the solid phase inside the reactor. When the experiment was performed, the capillaries were analysed again to compare with the initial solid state.

Once the reactor was closed with the basket inside, a sterilization step was carried out. A volume of 60 mL of demineralized water was injected, and a flush of N_2 gas was applied to eliminate O_2 in the reactor. The reactor was then heated to 100 °C for 24 h for sterilization under anoxic conditions. Afterwards, the reactor was cooled to 36 °C, which corresponded to the experimental temperature, and a light vacuum was created before the formation water was injected. The aqueous phase containing the autochthonous microorganisms was then injected into the reactor. Following the injection of the aqueous phase, the gaseous phase was added. The gas mixture initially consisted of CH_4 with 1% CO_2, 3.57 ppm benzene and 7.95 ppm toluene to simulate natural gas. Initially, the piston was at a high level such that the solid phase was completely immersed in the formation water. This step was important so that the solid phase came into contact with the aqueous phase and the microbial community. After 9 days, the piston was lowered, and only 1 cm of the solid phase remained in contact with the aqueous phase and in contact with microorganisms (2 cm in the gaseous phase). The gas mixture was reinjected to adjust for the loss of pressure. After 50 days, O_2 was injected into the system at a concentration of 100 ppm in the gas phase. The biotic experiment lasted 86 days. The basket containing the solid phase was carefully removed from the reactor and stored in a sealed anaerobic jar. An anaerobiosis generator and indicator pockets (Dutscher Ref. 0260001) were used in the jar. The basket was then transported to an anaerobic glove box. In the glove box, samples of the solid phase were collected for X-ray tomography and mineralogical analyses.

Thermodynamic modelling

To estimate the thermodynamic liquid–gas equilibrium, PhreeqC software was used to estimate the solubility of each gaseous compound in the system. To do so, a simplified abiotic system comprising the aqueous phase and the gas phase was modelled to quantify the solubility of the gas in the liquid phase at different stages of the experiment. The calculated values were then compared to the values measured with gas chromatography. The chosen database was 'Phreeqc.dat', which uses the extended Debye–Hückel law for the activity coefficient and the Redlich-type equation of state for the gas phase. Redox reactions were not taken into account due to their slow kinetics in such environments.[40–42] The calculated solubility corresponded to a simplified abiotic system in which only the gas and liquid phases were present. Estimating the dissolved gas in the aqueous phase helped to evaluate the amount of gases consumed by chemical reactions and microbial metabolism.

Results

Throughout the 86 days of the experiment, liquid and gas samples were collected and directly analysed by ion and gas chromatography, respectively. During the first 49 days, the system was under a pressure of 60 bar and a temperature of 36 °C, with a gaseous mixture composed of CH_4 and 1% CO_2 with traces of benzene and toluene. On day 50, O_2 was injected with a concentration of approximately 100 ppm in the gas phase. The results obtained during this experiment were divided into two main stages: before O_2 injection, when the simulated aquifer was under strict anoxic conditions similar to present-day conditions, and after O_2 injection, simulating the introduction of O_2 at a concentration equivalent to the maximum limit authorized today.

Evolution of the aqueous phase composition

The formation water sampled from the studied aquifer had very low salinity, approximately 0.8% of seawater salinity.[9,43] Underground sampling of the formation water showed that it contained $2.84 \times 10^{-2} \pm 1.5 \times 10^{-3}$ mmol of sulfate (ESI Table S1† and Fig. 1(a)). The sulfate quantity increased to $3.77 \times 10^{-1} \pm 1.9 \times 10^{-2}$ mmol after aqueous phase injection into the reactor due to solid–liquid interactions and compounds release from the solid phase. From day 9 to day 39, a decrease in dissolved sulfate was observed. After day 39 and until day 44, the sulfate quantity increased to $4.16 \times 10^{-1} \pm 2.1 \times 10^{-2}$ mmol after 0.1 μm-filtered wellhead water was added with sulfate into the system before O_2 injection. A decrease in sulfate quantity was then observed until day 51. Starting at this point, which corresponded to O_2 injection (day 50), the sulfate quantity was stable until the end of the experiment.

The acetate quantity was $1.16 \pm 5.0 \times 10^{-2}$ mmol at the beginning of the experiment (Fig. 1(b)). The concentration increased through the experiment to reach $1.64 \pm 8 \times 10^{-2}$ mmol on day 44. After O_2 injection, the acetate quantity reached a plateau around a value of $1.60 \pm 8 \times 10^{-2}$ mmol and stayed stable until the end of the experiment.

Evolution of the gas phase composition

After the injection of the aqueous phase into the reactor, the gas mixture of CH_4 + 1% CO_2 was added at a pressure of 60.6 ± 0.6 bar and a temperature of 36 °C to simulate the conditions in the targeted UGS. Using the PhreeqC model based on Peng–Robinson's equation, the compressibility factor of the gas mixture was calculated to be 0.9. Thus, by considering the compressibility factor, $4.45 \pm 2.2 \times 10^{-1}$ mol of CH_4 was injected at the beginning of the experiment (Fig. 2). After 3 days, the CH_4 quantity decreased from the gas phase and reached $4.40 \pm 2.2 \times 10^{-1}$ mol. As shown in Fig. 2, the calculated values of CH_4 corresponded to the quantity assumed to remain in the gas phase after thermodynamic equilibrium, based on PhreeqC calculations. On day 9, the piston's position was readjusted in the reactor to keep 1 cm of the solid phase immersed in the aqueous phase. After the piston level was lowered, the gas pressure was readjusted, and one more injection of the gas mixture was carried out. The gas injection induced an increase in CH_4 estimated to be approximately $3.07 \times 10^{-1} \pm 1.53 \times 10^{-2}$ mol. Until day 39, the quantity of CH_4 in the gas phase remained constant. After aqueous phase supplementation on

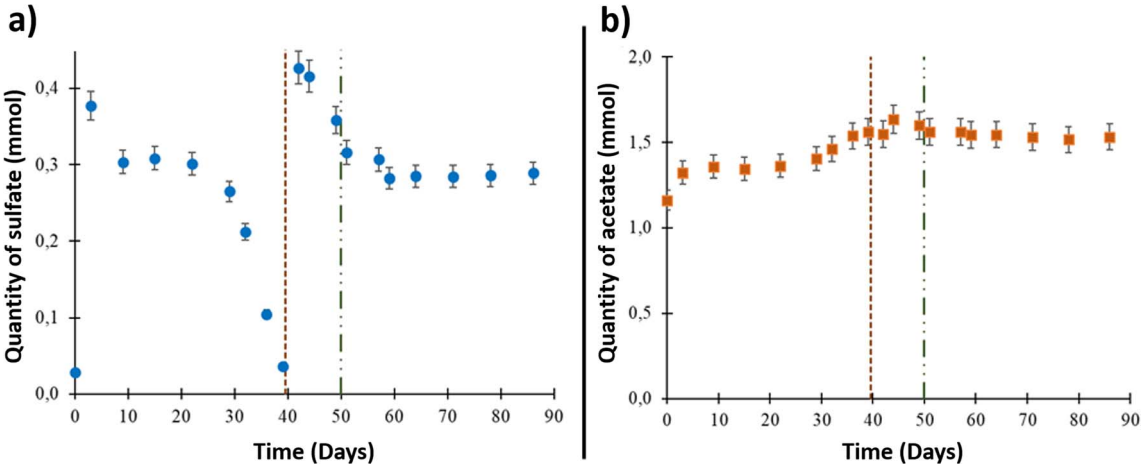

Fig. 1 Results of the aqueous phase analyses during the high-pressure experiment. The vertical dotted line on day 39 represents aqueous phase supplementation. The vertical line on day 50 represents oxygen injection. (a) Sulfate variation in the aqueous phase and (b) acetate variation in the aqueous phase.

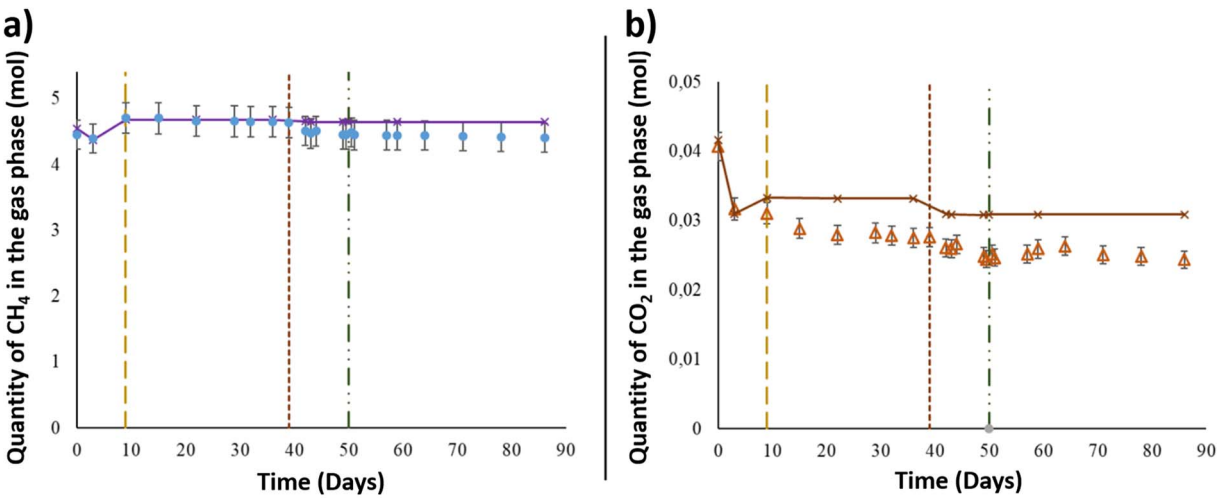

Fig. 2 Results of the gaseous phase analyses during the high-pressure experiment. The vertical dotted line on day 9 represents CH_4 + CO_2 reinjection. The vertical dotted line on day 39 represents aqueous phase supplementation. The vertical line on day 50 represents oxygen injection. (a) CH_4 variation in the gas phase. The purple dots and line represent the values calculated with PhreeqC. (b) CO_2 variation in the gas phase. The orange dots and line represent the values calculated with PhreeqC.

day 39, the CH_4 quantity in the gas phase decreased as it dissolved in the liquid phase. The quantity lost was $1.29 \times 10^{-1} \pm 6.47 \times 10^{-3}$ mol. Following the aqueous phase addition and the gas–liquid thermodynamic equilibrium, the quantity of CH_4 in the gas phase remained stable until the end of the experiment. The estimated CH_4 given by the thermodynamic model fit well with the experimental data obtained during the study (Fig. 2).

Along with methane, CO_2 was injected at the beginning of the experiment and was present in the gaseous mixture. Under a total pressure of 60.6 ± 0.6 bar and a temperature of 36 °C, the quantity of CO_2 initially injected into the system was $4.07 \times 10^{-2} \pm 2.0 \times 10^{-3}$ mol (Fig. 2), representing 1% of the gas phase. After thermodynamic equilibrium was reached between the gaseous and aqueous phases, a CO_2 decrease of $8.97 \times 10^{-3} \pm 4.5 \times 10^{-4}$ mol was observed from the initial quantity. Even with the reinjection of the gas mixture on day 9, the measured CO_2 quantity showed a decrease in the gas phase and was approximately $3.10 \times 10^{-2} \pm 1.5 \times 10^{-3}$ mol. The CO_2 quantity presented a continuous decrease through the experimental period to reach $2.47 \times 10^{-2} \pm 1.2 \times 10^{-3}$ mol on day 49, just before O_2 injection. Similar to CH_4, the calculated values of CO_2 represented the corresponding gas–liquid thermodynamic equilibrium in a binary abiotic system. As shown in Fig. 2, a marked difference was observed between the PhreeqC modelling results and experimental measurements, suggesting that the amount of gaseous CO_2 may be controlled by reactions other than aqueous phase dissolution, *e.g.*, microbial activity.

As explained above, the first step in the experiment was the reproduction of the aquifer conditions currently used for natural gas storage. The second step consisted of identifying the effects of O_2 presence in such ecosystems. The experimental conditions required an O_2 content of approximately 100 ppm in

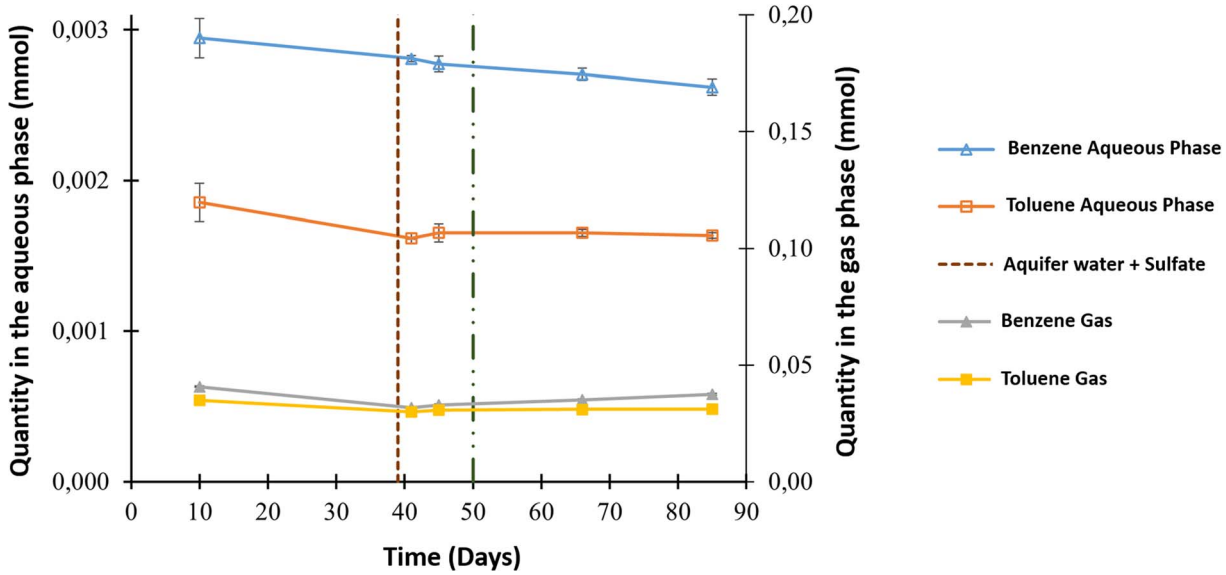

Fig. 3 Results of benzene and toluene variations in the gas and aqueous phases during the high-pressure experiment. The vertical dotted line on day 39 represents aqueous phase supplementation. The vertical line on day 50 represents oxygen injection. The blue and orange dots correspond to benzene and toluene values in the aqueous phase, respectively. The grey and yellow dots correspond to benzene and toluene values in the gas phase, respectively.

the gas phase, corresponding to the maximum quantity of O_2 authorized in UGS storage in France today. Since these low concentrations were measured using small gas samples in μ-GC, large uncertainties were generated in the measured values. The O_2 quantity in the gas phase varied between 70 and 170 ppm. The system became microoxic, and the O_2 content reached a plateau around this value. The solubility of O_2 calculated by PhreeqC was lower than 5.8×10^2 mM under these conditions. The redox potential increased in the formation water, confirming the presence of O_2 in the system (Fig. 4(a)).

The aqueous and gas phases were sampled throughout the experiment for additional analyses, such as benzene and toluene quantification. The main source of both compounds was the gaseous mixture that contained initial concentrations of 3.57 ppm benzene and 7.95 ppm toluene. Fig. 3 shows the evolution in the quantity of these compounds in both phases. Before O_2 injection, analyses of the aqueous phase showed a decrease in benzene from $2.95 \times 10^{-3} \pm 1.32 \times 10^{-4}$ to $2.77 \times 10^{-3} \pm 5.31 \times 10^{-5}$ mmol and toluene from $1.86 \times 10^{-3} \pm 1.26 \times 10^{-4}$ mmol to $1.65 \times 10^{-3} \pm 0.60 \times 10^{-4}$ mmol. A benzene decrease was also observed in the gas phase, with a value of approximately $7.79 \times 10^{-3} \pm 7.18 \times 10^{-4}$ mmol, but this was not the case for toluene. After the injection of O_2 into the system, benzene only decreased in the aqueous phase to reach $2.62 \times 10^{-3} \pm 5.39 \times 10^{-5}$ mmol; however, all the other values appeared to be constant.

Evolution of the microbial community

Members of the *Spirochaetaceae* family were detected throughout the experiment (Fig. 4(b)). Representing between 30 and 59% of the microbial community before the injection of O_2, their abundance decreased to reach 16% at the end of the experiment. Methanogenic archaea (*Methanobacteriaceae*, *Methanothermobacteriaceae*, *Methanosaetaceae* and *Methanosarcinaceae*), which represented nearly 19% of the diversity at the beginning of the experiment, drastically decreased after the 36th day of incubation and O_2 injection, while the new equilibrium within the community favoured bacteria involved in the sulfur cycle. The *Desulfurisporaceae* family represented up to 39% of the community on day 36 and was most active (Fig. 4(c)). With the decrease in sulfate, the family *Desulfurisporaceae* (*Desulfurispora* genus) and its activity decreased from the 36th to the 42nd day. Supplementation with sulfate did not allow their regrowth before the injection of O_2 on the 50th day. On the other hand, the reduction of sulfates and the injection of O_2 did not impact the growth of *Desulfitibacteraceae*, which were part of the dominant families. The members of this family identified in this study are all affiliated with the genus *Desulfosporosinus*. The injection of O_2 allowed a strong development of bacteria belonging to the class Acidobacteriae, which represented 64% of the microbial community at the end of the experiment. Acidobacteriae genes were very active and dominated the *16S rRNA* gene transcripts (Fig. 4(c)). To a lesser extent, these new conditions also favoured the development of members of the *Kineosporiaceae* family (9% at the end of the experiment; affiliated with the genus *Quadrisphaera*). Although the low concentration of O_2 in the gas phase made O_2 quantification difficult, its presence led to an increase in the redox potential of the aqueous phase from approximately −160 mV before the injection of O_2 to +73 mV at the end of the experiment (Fig. 4(a)). In addition, this introduction of O_2 quickly stopped the decrease in sulfate in the 10 days that followed. The sulfate content was stable until the end of the experiment, clearly indicating the cessation of sulfate reduction, which was corroborated by the disappearance of the *dsrB*

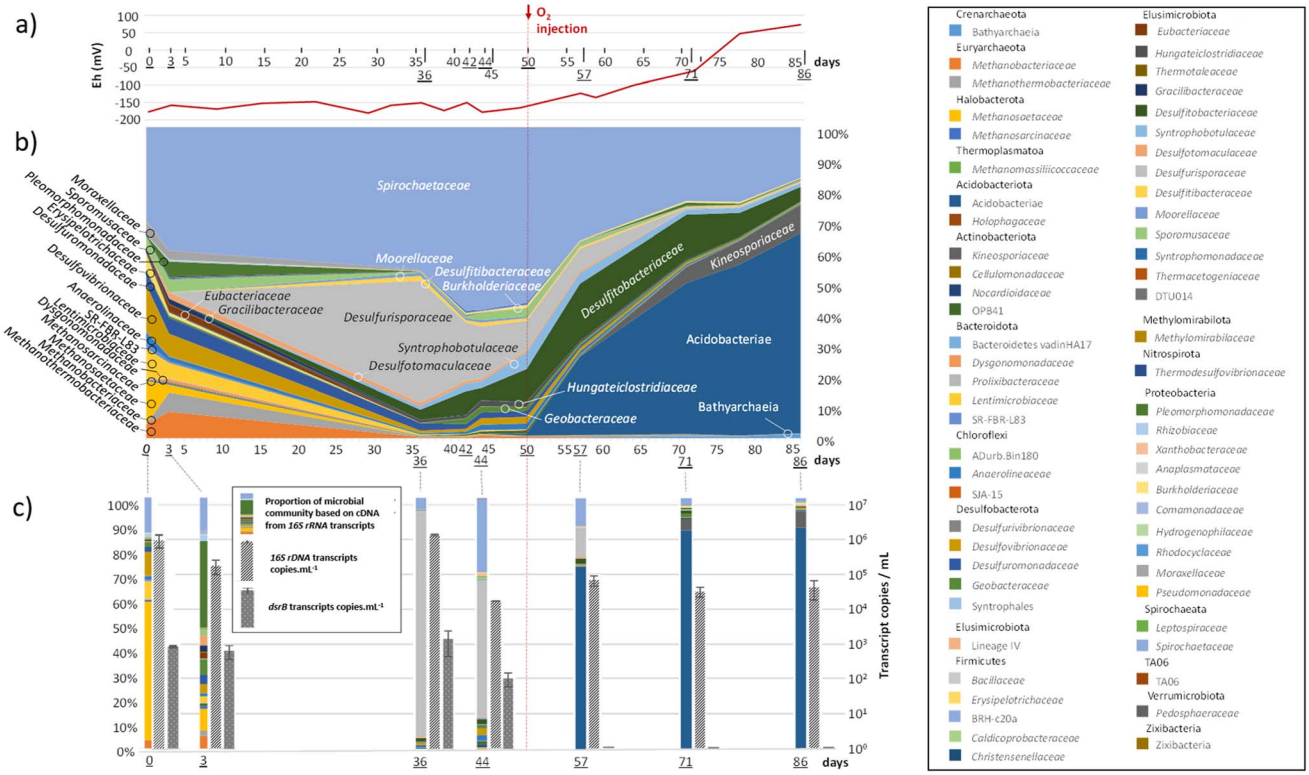

Fig. 4 Temporal monitoring of microbial community evolution during the experiment simulating gas (CH_4, 1% CO_2) storage in a deep aquifer under 60 bar and 36 °C conditions. The vertical dotted line separates samples collected before and after the injection of approximately 100 ppm O_2 on the 50th day of incubation. (a) Redox potential (mV) monitored throughout the experiment. (b) Tracking the taxonomic diversity of the microbial community at the family level based on the *16S rRNA* gene. (c) Monitoring active taxonomic diversity of the microbial community based on *16S rRNA* gene transcripts (relative quantification) and absolute RT-qPCR quantification of *16S rRNA* gene transcripts (v4–v5) and *dsrB* (diversity of sulfate reducers) gene transcripts.

transcripts. The quantification results of the *16S rRNA* gene transcripts (Fig. 4(c)) corresponded well to the observations made from DNA (Fig. 4(b)) and showed that although the microbial community evolved, it maintained its activity throughout the experiment ($1.83 \times 10^4 \pm 1.14 \times 10^2$ to $1.50 \times 10^6 \pm 7.26 \times 10^4$ *16S rRNA* transcript copies per mL). In addition, *16S rRNA* gene concentration monitoring indicated a microorganism concentration of $3.93 \times 10^5 \pm 1.31 \times 10^4$ *16S rRNA* gene copies per mL at the start of the experiment and $1.51 \times 10^5 \pm 2.26 \times 10^4$ *16S rRNA* gene copies per mL at the end of the experiment (ESI Table S2†). Throughout the experiment, *mcrA* genes were detected in small quantities in the sampled aqueous phase. However, transcripts showed that those microorganisms were not active (Fig. 4(c)). At the end of the experiment, 96% of the microbial community was dominated by 6 microbial taxonomic groups: the class Acidobacteriae (64%), the family *Spirochaetaceae* (16%), the family *Kineosporiaceae* (9%), the family *Desulfitobacteriaceae* (5%), the class Bathyarchaeia (1%) and the family *Syntrophobotulaceae* (1%). Close OTUs of the Acidobacteriae class were related to environmental sequences (accession number: AF407714; 375 nt/99.7% identity and acc#: KP676769; 375 nt/99.7%) from Australia's Great Artesian Basin (52 °C) and Russian hot springs. OTUs affiliated with the *Spirochaetaceae* family were related to bacteria, in particular *Rectinema cohabitans*, from microbial communities degrading aromatic hydrocarbons (acc#: JF800779; AY214182; KP297860). OTUs related to the family *Kineosporiaceae* were affiliated with a bacterium described to have phosphate-solubilization activity[44] (NII-1013). OTUs grouped in the *Desulfitobacteriaceae* family were affiliated with the genus *Desulfosporosinus*, with environmental sequences found in deep (acc#: KX822015, MF942638, JX470444, *etc.*) and acidic (acc#: DQ137901, GY127803, GQ342329, *etc.*) ecosystems. OTUs clustered in the class Bathyarchaeia were related to environmental sequences detected in consortia involved in the degradation and fermentation of organic matter (acc# CU916921; KJ424517; U81774). Finally, close OTUs of the *Syntrophobotulaceae* family were affiliated with environmental sequences of deep aquifers (acc#: LC198569).

Evolution of the solid phase from the beginning to end of the experiment

Analyses of the reservoir rock before and after the experiment were carried out to identify potential changes in mineral phases and porosity. X-ray diffraction patterns identified quartz as the dominant phase (81%), while calcite was also present (12%) at the beginning and at the end of the experiment (Fig. S2†). Clay minerals were detected as minor phases (kaolinite and illite < 2%) as well as muscovite (<4%). Iron sulfides such as marcasite were possibly present as trace phases. The results confirmed that the

reservoir rock was mainly composed of quartz, with a minor presence of calcite and clay minerals.[9] Furthermore, samples analysed by scanning electron microscopy (SEM) showed the additional presence of feldspars. Ti-oxide minerals (likely rutile), as well as rare zircon and gypsum crystals, were initially contained in the reservoir rock. At the end of the experiment, no substantial changes were identified except the formation of microcrystals containing zinc oxides, which was observed by SEM-EDS.

Similarly, X-ray tomography was conducted on samples before and after the experiment. The analyses did not reveal any morphological alterations of the solid phase. The grey level of the aqueous phase did, however, exhibit slight variations by the end of the test. Such a difference can be a proxy for the presence of microorganisms. In fact, although microorganisms are principally composed of water, their density[45] (between 1 and 1.05) endows them with a slightly higher attenuation coefficient than that of the surrounding water. As a consequence, microorganisms appear slightly brighter in reconstructed images. To further explore this observation, the voxels constituting the water phase were separated into higher and lower attenuating classes, corresponding to brighter and darker pixels, respectively. The threshold between the two classes was set to the average grey level of all voxels constituting the water phase. The median value was also tested and yielded very similar results.

Fig. S3† depicts three orthogonal cuts through one of the obtained datasets. The images were colour-coded, where red was the solid grains, blue was the water phase and grey was the gas phase. It was immediately clear that the water phase mainly remained at the bottom of the sample, while the gas phase was mainly found in the upper portion of the capillary. The interface between the two phases was not flat, as it resulted from the complex interplay between capillary forces and gravity. In the water phase, the presence of small green areas was noted. This corresponded to the region where higher attenuation was found, which was explained by a higher-than-average concentration of microorganisms. As observed, microorganisms were concentrated in areas close to the grains, and the centres of the pores remained vacant.

Discussion

Similar to natural gas, massive amounts of biomethane are planned to be stored in UGS such as salt cavities and deep aquifers.[9,46] In this paper, the influence of a 100 ppm O_2 injection into deep aquifers was studied, particularly its impact on the microbial life. In fact, many studies have confirmed and presented a direct effect of O_2 on autochthonous microbial communities.[9,13,26] The same study site with the code name Ab_L_1 was used to study the impact of 1% O_2 on biomethane storage.[47] The aqueous phase had very low salinity, less than 0.8% of marine water salinity. During the experiment, the system was maintained under anoxic conditions for 49 days. O_2 was injected on day 50, and the system was further studied for 36 days.

Evolution of the system before O_2 injection

During the first phase of the experiment, the reactor represented an UGS of natural gas at 60 bar and 36 °C. For 49 days, the liquid, gas and solid phases and microorganisms interacted and a decrease in benzene and toluene was observed in the liquid phase (Fig. 3). During the first days, the sulfate content slightly increased in the aqueous phase. Initially, the measured sulfate in the aqueous phase was very low at approximately $2.85 \times 10^{-2} \pm 1.42 \times 10^{-3}$ mmol. Once in contact with the solid phase, this quantity increased and reached $3.37 \times 10^{-1} \pm 1.89 \times 10^{-2}$ mmol. Based on the reservoir rock analyses, the increase in the sulfate content may be explained by the dissolution of gypsum ($CaSO_4$) as identified by SEM-EDS or barium sulfate ($BaSO_4$) as detected by XRD (Fig. S3†) or from residual drilling brines contained in the pores (some might have remained even though the rock was washed with demineralized water). The same results and sulfate increase were obtained in previous experiments using aquifer reservoir rock.[9,10] After the increase, a consumption of sulfate was observed in the system until complete depletion on day 39. This observation reoccurred after sulfate supplementation on day 39, and the sulfate content decreased again under anoxic conditions (Fig. 1(a)). Furthermore, previous studies on the Ab_L_1 aquifer identified SRM activity and provided evidence for the presence of the *Desulfovibrionaceae* family.[4,47]

The presence of a necromass in the microbial community co-injected with the formation water in the HP reactor could explain the growth of SRM such as those belonging to the *Desulfovibrionaceae* family and fermentative microorganisms such as *Spirochaetaceae*, which lead to the production of organic acids such as acetate, CO_2 and H_2. These compounds could benefit the growth of methanogenic archaea and lead to the potential disappearance of sulfate (Fig. 4(b)). In fact, the *Methanobacteriaceae* and *Methanothermobacteriaceae* families include microorganisms described to be hydrogenotrophic, while the *Methanosaetaceae* and *Methanosarcinaceae* families include acetotrophs and methylotrophs.[48] Fermentation continued during the first 20 days of incubation and potentially produced H_2.[49] Therefore, autotrophic metabolisms explain why the observed gaseous phase value of CO_2 was lower than the theoretical value predicted from CO_2 dissolution into the aqueous phase (Fig. 2). The thermodynamic calculations using the PhreeqC model based on an abiotic binary system suggested that other phenomena contributed to the experimentally observed disappearance of CO_2. Some microorganisms identified in this study at the start of the experiment, *e.g.*, *Methanobacteriaceae* and *Methanothermobacteriaceae*, and a few *Desulfovibrionaceae*, which have lithoautotrophic metabolisms that employ H_2 (from fermentation) as an energy and electron source and CO_2 as an electron acceptor and carbon source for biomass production, could have played such a role in CO_2 removal.

Among the SRMs, the physicochemical conditions and the presence of rock seemed to have favoured the growth and activity of the genus *Desulfurispora*, which are known to incompletely oxidize organic substrates to acetate.[50] The quantity of the latter increased in the liquid phase before the injection of O_2 (Fig. 1(b), 4(b and c)). Since fermenters such as *Spirochaetaceae* and SRMs such as *Desulfurisporaceae* were not competitors for electron acceptors, the high relative decrease in the activity of *Spirochaetaceae* observed on the 36th day could be due to a decrease in the concentrations of accessible organic

substrates in the reactor. From the 36th day, the decrease in the quantity of sulfate (<1 mmol) and the probable limitation in organic substrates seemed to favour the members of the *Desulfitobacteriaceae* family to the detriment of the *Desulfurisporaceae* family.

Evolution of the system after O_2 injection

As part of the experiment, 100 ppm O_2 was injected into the gas phase on the 50th day of incubation. It is important to specify that the rock material of the targeted UGS site consisted mainly of quartz, which poorly reacts with oxygen. Only a limited amount of O_2 could have been trapped *a priori* following mineral oxidation. Therefore, the effects were mainly observed in the liquid phase and the microbial community. Injection had several effects: (i) an increase in the redox potential to +73 mV; (ii) cessation of sulfate reduction and stabilization at $2.82 \times 10^{-1} \pm 1.41 \times 10^{-2}$ mmol until the end of the experiment (40 days); (iii) cessation of the appearance of acetate and stabilization of its concentration at $1.56 \pm 7.80 \times 10^{-2}$ mmol; (iv) cessation in the disappearance of CO_2 from the gaseous phase. These four effects were explained by the community modifications induced by the introduction of O_2. SRMs that are under strictly anoxic conditions suffered from oxygen toxicity. Under conditions simulating the aquifer (60 bar and 36 °C), the O_2 concentration was estimated by calculations to be approximately 5.8×10^{-2} mM in the aqueous phase. Two days after the injection of O_2, *Desulfurisporaceae* represented only a small portion of the active microorganisms (Fig. 4(c)). The apparent antagonism between the disappearance of sulfate-reducing activity demonstrated by the absence of *dsrB* transcripts and the identification of numerous SRMs affiliated with the *Desulfitobacteriaceae* family (*i.e.*, *Desulfosporosinus* sp.) may explain the versatility of their metabolism and their ability to ferment or use other terminal electron acceptors.[51] These microorganisms have been identified in groundwater contaminated with BTEX and are regularly shown to be key players in the biodegradation of these monoaromatic hydrocarbons.[52–56] Interestingly, it seems that the cessation of sulfate reduction following O_2 injection did not slow the degradation of benzene in our experiment, which could be explained by the microbes' ability to ferment this compound.[57] The taxonomic group that was mainly favoured by the new conditions included bacteria affiliated with the class Acidobacteriae, which account for more than 80% of the microbial activity (Fig. 4(c)). The development of these taxonomic groups (*Desulfosporosinus* and Acidobacteriae) is not surprising since they are associated with acidic pH conditions.[51,58] Although the pH could not be monitored in this experiment, the work of Sin and her collaborators[25] in another storage aquifer showed that the injection of O_2 and the presence of CO_2 led to an acidification of the formation water due to the dissolution of certain minerals such as pyrite. Slight acidification has previously been shown to be conducive to the biodegradation of BTEX.[5,10] Finally, the new microoxic conditions also allowed the development of members of the *Kineosporiaceae* family (*Quadrisphaera* spp.), which are described as aerobic microorganisms[59] but can be assumed to be able to ferment to maintain themselves in deep anoxic aquifers since they are unable to sporulate.

At the end of the experiment, the solid phase demonstrated no substantial changes except for the formation of microcrystals containing oxides (ESI Fig. S2†). X-ray tomography scans confirmed the absence of significant alterations (ESI Fig. S3†). Therefore, even though ionic compounds were released into the aqueous phase, the nature of the reservoir rock, which was mainly composed of quartz, was not strongly impacted by the O_2 injection. Finally, X-ray data provided a strong indication that microorganisms were not distributed uniformly throughout the aqueous phase but rather clustered in close proximity to grain boundaries.

Conclusions

Biomethane storage in underground aquifers is a mandatory step to ensure the energy transition and to substitute natural gas. During our experimental study, a deep aquifer situated in France was reproduced in a high-pressure reactor under a pressure of 60 bar and a temperature of 36 °C. As designed, the reactor cannot simulate a continuous flow of water in the rock, as in the aquifer. However, a small amount of water is displaced as the piston moves to rebalance the pressure following the various withdrawals during the experiment. Finally, we believe that we are very close to the reality, since the movement of the formation water is very slight (of the order of a meter or a few meters per year). To summarize the effects observed after the injection of 100 ppm of O_2 in the biomethane mixture:

- The cessation of bacterial sulfate reduction and a change in the microbial community were detected. O_2's effect on the microbial community was not limited to sulfate reducers only, but greater changes occurred.
- Even though the ecosystem varied, the biodegradation of benzene was maintained.
- Conversely, no remarkable changes were observed in the solid phase.
- The same on the gas phase initially composed of CH_4 with 1% CO_2, and decrease of the latter one was detected. CO_2 consumption was related to microbial activity as their source of carbon. Thus once the amount of O_2 was injected and the microbial activity became very slow, CO_2 consumption stopped.

Shifts in the microbial community due to O_2 injection can have larger impacts on aquifer's evolution and stability. In fact, existing and active microorganisms in the aquifers today are responsible to degrade hydrocarbons present *in situ*. Studying the effect of O_2 as an impurity during biomethane storage has an added value to fix the O_2 limit in biomethane. Here, injecting 100 ppm O_2 into a UGS in a deep aquifer does not appear to affect its operation. These results compose developed knowledge about O_2 biological geological and chemical impact on the underground. The effects of O_2 on UGS must be correlated with O_2 effects on the gas network facilities used today. Findings can be used in any other process including O_2 as an impurity such as CCS and CAES. Further studies applied on aquifer storage are needed to dissect the multiple results of our findings in order to optimize O_2 injection in the underground and possibly increase

the regulatory limits for O_2 to enhance the development of the biomethane sector in Europe.

Abbreviations

BTEX:	Benzene, toluene, ethylbenzene, xylene
CAES:	Compressed air energy storage
CCS:	Carbon capture and storage
CH_4:	Methane
CO_2:	Carbon dioxide
H_2	Hydrogen
H_2S	Hydrogen sulfide
HP	High pressure
N_2	Nitrogen
O_2	Dioxygen
SRM	Sulfate reducing microorganisms
UGS	Underground gas storage

Author contributions

FC, MRP, PC and ARP co-conceived the study. PH, JM, FC, and PC carried out the high pressure and simulation experiments. MG, MRP and ARP applied the microbiological approaches. PS, M-PI, PM and GH used the imaging and mineralogical characterization. ML and ILH analyzed the hydrocarbons. All authors contributed to the interpretation of results and paper writing.

Conflicts of interest

PCh, GC and AP are employed by two French companies specialized in geological natural gas storage, which are Teréga and Storengy, respectively.

Acknowledgements

Enagas, SNAM, Storengy and Teréga are acknowledged for funding this research project. We are grateful to the Genotoul platform (**https://genotoul.fr**) for the sequencing analyses. MRP salary was supported by E2S-UPPA. We would also like to thank TotalEnergies for providing UMS 3360 DMEX with the Zeiss Xradia Versa 510, which carried out the tomographic acquisitions reported in this article.

References

1 Ministères Ecologie Energie Territoires, *Accélération des énergies renouvelables : le Gouvernement prend deux mesures réglementaires pour accroître la capacité de production de biométhane en France*, 2022, **https://www.ecologie.gouv.fr/acceleration-des-energies-renouvelables-gouvernement-prend-deux-mesures-reglementaires-accroitre**, accessed 10.10.22.

2 C. De Lorgeril, *European Biomethane Benchmark*, SIA Partners, 2022.

3 C. Magnabosco, K. Ryan, M. C. Y. Lau, O. Kuloyo, B. Sherwood Lollar, T. L. Kieft, E. van Heerden and T. C. Onstott, A metagenomic window into carbon metabolism at 3 km depth in Precambrian continental crust, *ISME J.*, 2016, **10**, 730–741.

4 M. Ranchou-Peyruse, J.-C. Auguet, C. Mazière, C. X. Restrepo-Ortiz, M. Guignard, D. Dequidt, P. Chiquet, P. Cézac and A. Ranchou-Peyruse, Geological gas-storage shapes deep life, *Environ. Microbiol.*, 2019, **21**(10), 3953–3964.

5 S. Berlendis, J.-F. Lascourreges, B. Schraauwers, P. Sivadon and M. Magot, Anaerobic biodegradation of BTEX by original bacterial communities from an underground gas storage aquifer, *Environ. Sci. Technol.*, 2010, **44**, 3621–3628.

6 P. Bombach, A. Chatzinotas, T. R. Neu, M. Kästner, T. Lueders and C. Vogt, Enrichment and characterization of a sulfate-reducing toluene-degrading microbial consortium by combining in situ microcosms and stable isotope probing techniques, *FEMS Microbiol. Ecol.*, 2010, **71**, 237–246.

7 J. Detmers, H. Strauss, U. Schulte, A. Bergmann, K. Knittel and J. Kuever, FISH shows that Desulfotomaculum spp. are the dominating sulfate-reducing bacteria in a pristine aquifer, *Microb. Ecol.*, 2004, **47**(3), 236–242.

8 N. K. Fry, J. K. Fredrickson, S. Fishbain, M. Wagner and D. A. Stahl, Population structure of microbial communities associated with two deep, anaerobic, alkaline aquifers, *Appl. Environ. Microbiol.*, 1997, **63**, 1498–1504.

9 P. G. Haddad, J. Mura, F. Castéran, M. Guignard, M. Ranchou-Peyruse, P. Sénéchal, M. Larregieu, M.-P. Isaure, I. Svahn, P. Moonen, I. Le Hécho, G. Hoareau, P. Chiquet, G. Caumette, D. Dequidt, P. Cézac and A. Ranchou-Peyruse, Biological, geological and chemical effects of oxygen injection in underground gas storage aquifers in the setting of biomethane deployment, *Sci. Total Environ.*, 2022, **806**(pt 3), 150690.

10 P. G. Haddad, M. Ranchou-Peyruse, M. Guignard, J. Mura, F. Castéran, L. Ronjon-Magand, P. Senechal, M.-P. Isaure, P. Moonen, G. Hoareau, D. Dequidt, P. Chiquet, G. Caumette, P. Cézac and A. Ranchou-Peyruse, Geological storage of hydrogen in deep aquifers – an experimental multidisciplinary study, *Energy Environ. Sci.*, 2022, **15**, 3400–3415.

11 M. Itävaara, M. Nyyssönen, A. Kapanen, A. Nousiainen, L. Ahonen and I. Kukkonen, Characterization of Bacterial Diversity to a Depth of 1500 m in the Outokumpu Deep Borehole, Fennoscandian Shield: Deep Terrestrial Biodiversity, *FEMS Microbiol. Ecol.*, 2011, **77**, 295–309.

12 M. Ranchou-Peyruse, M. Guignard, F. Castéran, M. Abadie, C. Defois, P. Peyret, D. Dequidt, G. Caumette, P. Chiquet, P. Cézac and A. Ranchou-Peyruse, Microbial diversity under the influence of natural gas storage in a deep aquifer, *Front. Microbiol.*, 2021, **12**, 688929.

13 H. Morgan, D. J. Large, K. Bateman, D. Hanstock and S. P. Gregory, Potential impacts of oxygen impurities in carbon capture and storage on microbial community composition and activity, *Int. J. Greenhouse Gas Control*, 2021, **111**, 103479.

14 T. Aüllo, S. Berlendis, J.-F. Lascourrèges, D. Dessort, D. Duclerc, S. Saint-Laurent, B. Schraauwers, J. Mas,

D. Patriarche, C. Boesinger, M. Magot and A. Ranchou-Peyruse, New bio-indicators for long term natural attenuation of monoaromatic compounds in deep terrestrial aquifers, *Front. Microbiol.*, 2016, **7**, 122.

15 M. Ranchou-Peyruse, C. Gasc, M. Guignard, T. Aüllo, D. Dequidt, P. Peyret and A. Ranchou-Peyruse, The sequence capture by hybridization: a new approach for revealing the potential of mono-aromatic hydrocarbons bioattenuation in a deep oligotrophic aquifer, *Microb. Biotechnol.*, 2017, **10**, 469–479.

16 D. Barik, S. Sah and S. Murugan, Biogas production and storage for fueling internal combustion engines, *Int. J. Emerging Technol. Adv. Eng.*, 2013, **3**(3), 193–202.

17 E. de Visser, C. Hendriks, M. Barrio, M. J. Mølnvik, G. de Koeijer, S. Liljemark and Y. Le Gallo, Dynamics CO2 quality recommendations, *Int. J. Greenhouse Gas Control*, 2008, **2**, 478–484.

18 M. D. Jensen, *CO2 Transport*, IEAGHG 10th International CCS Summer School, Regina, Canada, 2016.

19 EASEE-Gas, *Common Business Practice*, 2005, 2005-001/02, **https://easee-gas.eu/download_file/DownloadFile/4/cbp-2005-001-02-harmonisation-of-natural-gas-quality/**, accessed on 1 December 2019.

20 M. Koenen, T. J. Tambach and F. P. Neele, Geochemical effects of impurities in CO2 on a sandstone reservoir, *Energy Procedia*, 2011, **4**, 5343–5349.

21 H. Morgan, D. Large, K. Bateman, D. Hanstock and S. Gregory, The effect of variable oxygen impurities on microbial activity in conditions resembling geological storage sites, *Energy Procedia*, 2017, **114**, 3077–3087.

22 H. P. Vu, J. R. Black and R. R Haese, The geochemical effects of O2 and SO2 as CO2 impurities on fluid-rock reactions in a CO2 storage reservoir, *Int. J. Greenhouse Gas Control*, 2018, **68**, 86–98.

23 C. Guo, C. Li, K. Zhang, Z. Cai, T. Ma, F. Maggi, Y. Gan, A. El-Zein, Z. Pan and L. Shen, The promise and challenges of utility-scale compressed air energy storage in aquifers, *Appl. Energy*, 2021, **286**, 116513.

24 R. Kushnir, A. Ullmann and A. Dayan, Thermodynamic and hydrodynamic response of compressed air energy storage reservoirs: a review, *Rev. Chem. Eng.*, 2012, **28**, 123–148.

25 I. Sin, L. De Windt, C. Banc, P. Goblet and D. Dequidt, Assessment of the oxygen reactivity in a gas storage facility by multiphase reactive transport modeling of field data for air injection into a sandstone reservoir in the Paris Basin, France, *Sci. Total Environ.*, 2023, **17**, 161657.

26 M. Cai, C. Yu, R. Wang, Y. Si, K. Masakorala, H. Yuan, J. Yao and J. Zhang, Effects of oxygen injection on oil biodegradation and biodiversity of reservoir microorganisms in Dagang oil field, China, *Int. Biodeterior. Biodegrad.*, 2015, **98**, 59–65.

27 Y.-F. Liu, D. D. Galzerani, S. M. Mbadinga, L. S. Zaramela, J.-D. Gu, B.-Z. Mu and K. Zengler, Metabolic capability and in situ activity of microorganisms in an oil reservoir, *Microbiome*, 2018, **6**, 5.

28 M. Pannekens, L. Kroll, H. Müller, F. T. Mbow and R. U. Meckenstock, Oil reservoirs, an exceptional habitat for microorganisms, *New Biotechnol.*, 2019, **49**, 1–9.

29 P. J. Lien, Z. H. Yang, Y. M. Chang, Y. T. Tu and C. M. Kao, Enhanced bioremediation of TCE-contaminated groundwater with coexistence of fuel oil: effectiveness and mechanism study, *Chem. Eng. J.*, 2016, **289**, 525–536.

30 E. Trulli, C. Morosini, E. Rada and V. Torretta, Remediation in situ of hydrocarbons by combined treatment in a contaminated alluvial soil due to an accidental spill of LNAPL, *Sustainability*, 2016, **8**(11), 1086.

31 H. B. Jung, W. Um and K. J. Cantrell, Effect of oxygen co-injected with carbon dioxide on Gothic shale caprock–CO2–brine interaction during geologic carbon sequestration, *Chem. Geol.*, 2013, **354**, 1–14.

32 J. Lu, P. J. Mickler, J.-P. Nicot, C. Yang and R. Darvari, Geochemical impact of O2 impurity in CO2 stream on carbonate carbon-storage reservoirs, *Int. J. Greenhouse Gas Control*, 2016, **47**, 159–175.

33 M. Ranchou-Peyruse, M. Guignard, P. G. Haddad, S. Robin, M. Lanot, H. Carrier, D. Dequidt, P. Chiquet, P. Cézac and A. Ranchou-Peyruse, A deep continental aquifer downhole sampler for microbiological studies, *Front. Microbiol.*, 2023, **13**, 1012400.

34 Y. Wang and P.-Y. Qian, Conservative fragments in bacterial 16S rRNA genes and primer design for 16S ribosomal DNA amplicons in metagenomic studies, *PLoS One*, 2009, **4**, e7401.

35 F. Escudié, L. Auer, M. Bernard, M. Mariadassou, L. Cauquil, K. Vidal, S. Maman, G. Hernandez-Raquet, S. Combes and G. Pascal, FROGS: Find, Rapidly, OTUs with Galaxy Solution, *Bioinformatics*, 2018, **34**, 1287–1294.

36 J. Geets, B. Borremans, L. Diels, D. Springael, J. Vangronsveld, D. van der Lelie and K. Vanbroekhoven, dsrB gene-based DGGE for community and diversity surveys of sulfate-reducing bacteria, *J. Microbiol. Methods*, 2006, **66**, 194–205.

37 M. Wagner, A. J. Roger, G. Brusseau and D. A. Stahl, Phylogeny of dissimilatory sulfite reductases supports an early origin of sulfate respiration, *J. Bacteriol.*, 1998, **180**, 2975–2982.

38 L. M. Steinberg and J. M. Regan, Phylogenetic comparison of the methanogenic communities from an acidic, oligotrophic fen and an anaerobic digester treating municipal wastewater sludge, *Appl. Environ. Microbiol.*, 2008, **74**, 6663–6671.

39 L. M. Steinberg and J. M. Regan, mcrA-targeted real-time quantitative PCR method to examine methanogen communities, *Appl. Environ. Microbiol.*, 2009, **75**, 4435–4442.

40 R. D. Lindberg and D. D. Runnells, Ground water redox reactions: an analysis of equilibrium state applied to Eh measurements and geochemical modelling, *Science*, 1984, **225**, 925–927.

41 A. Stefánsson, S. Arnórsson and Á. E. Sveinbjörnsdóttir, Redox reactions and potentials in natural waters at disequilibrium, *Chem. Geol.*, 2005, **221**, 289–311.

42 D. C. Thorstenson, Equilibrium distribution of small organic molecules in natural waters, *Geochim. Cosmochim. Acta*, 1970, **34**, 745–770.

43 D. Banks, Y. A. Frank, V. Kadnikov, O. V. Karnachuk, M. J. Watts A. J. Boyce and B. Frengstad, *Hydrochemical Data Report from Sampling of Two Deep Abandoned Hydrocarbon Exploration Wells: Byelii Yar and Parabel', Tomsk Oblast', Western Siberia, Russian Federation, Report No. 2014.034*, Geological Survey of Norway, 2014.

44 S. G. Dastager and S. Damare, Marine Actinobacteria showing phosphate-solubilizing efficiency in Chorao Island, Goa, India, *Curr. Microbiol.*, 2013, **66**, 421–427.

45 A. J. Sawyer, M. H. Griggs and R. Wayne, Dimensions, density, and settling velocity of entomophthoralean Conidia: implications for aerial dissemination of spores, *J. Invertebr. Pathol.*, 1994, **63**, 43–55.

46 M. Torrijos, State of development of biogas production in Europe, *Procedia Environ. Sci.*, 2016, **35**, 881–889.

47 P. Haddad, A. Ranchou-Peyruse, P. Cézac, F. Casteran, M. Guignard, P. Chiquet, G. Caumette and D. Dequidt, *Research on the Injection of New Gases in Underground Methane Storage Systems in Deep Aquifers, Goldschmidt Conference*, Virtual, 2021.

48 B. Demirel and P. Scherer, The roles of acetotrophic and hydrogenotrophic methanogens during anaerobic conversion of biomass to methane: a review, *Rev. Environ. Sci. Biotechnol.*, 2008, **7**, 173–190.

49 X. Wu, K. Holmfeldt, V. Hubalek, D. Lundin, M. Åström, S. Bertilsson and M. Dopson, Microbial metagenomes from three aquifers in the Fennoscandian shield terrestrial deep biosphere reveal metabolic partitioning among populations, *ISME J.*, 2016, **10**(5), 1192–1203.

50 M. Watanabe, M. Fukui and J. Kuever, *Bergey's Manual of Systematics of Archaea and Bacteria, Desulfurisporaceae fam. nov.*, John Wiley & Sons, New York, 2020, pp. 1–2.

51 M. Pester, E. Brambilla, D. Alazard, T. Rattei, T. Weinmaier, J. Han, S. Lucas, A. Lapidus, F. J. Cheng, L. Goodwin, S. Pitluck, L. Peters, G. Ovchinnikova, H. Teshima, J. C. Detter, C. S. Han, R. Tapia, M. L. Land, L. Hauser, N. C. Kyrpides, N. N. Ivanova, I. Pagani, M. Huntmann, C. L. Wei, K. W. Davenport, H. Daligault, P. S. Chain, A. Chen, K. Mavromatis, V. Markowitz, E. Szeto, N. Mikhailova, A. Pati, M. Wagner, T. Woyke, B. Ollivier, H. P. Klenk, S. Spring and A. Loy, Complete genome sequences of Desulfosporosinus orientis DSM765T, Desulfosporosinus youngiae DSM17734T, Desulfosporosinus meridiei DSM13257T, and Desulfosporosinus acidiphilus DSM22704T, *J. Bacteriol.*, 2012, **194**(22), 6300–6301.

52 N. A. Laban, B. Tan, A. Dao and J. Foght, Draft genome sequence of uncultivated Desulfosporosinus sp. strain Tol-M, obtained by stable isotope probing using [13C6]toluene, *Genome Announc.*, 2015, **3**(1), e01422.

53 U. Kunapuli, T. Lueders and R. U. Meckenstock, The use of stable isotope probing to identify key iron-reducing microorganisms involved in anaerobic benzene degradation, *ISME J.*, 2007, **7**, 643–653.

54 W. J. Robertson, J. P. Bowman, P. D. Franzmann and M. J. Mee, Desulfosporosinus meridiei sp. nov., a spore-forming sulfate-reducing bacterium isolated from gasolene-contaminated groundwater, *Int. J. Syst. Evol. Microbiol.*, 2001, **51**, 133–140.

55 W. Sun, X. Sun and A. M. Cupples, Identification of Desulfosporosinus as toluene-assimilating microorganisms from a methanogenic consortium, *Int. Biodeterior. Biodegrad.*, 2014, **88**, 13–19.

56 C. Winderl, H. Penning, F. Netzer, R. U. Meckenstock and T. Lueders, DNA-SIP identifies sulfate-reducing Clostridia as important toluene degraders in tar-oil-contaminated aquifer sediment, *ISME J.*, 2010, **4**(10), 1314–1425.

57 D. T. Ramos, M. L. da Silva, H. S. Chiaranda, P. J. Alvarez and H. X. Corseuil, Biostimulation of anaerobic BTEX biodegradation under fermentative methanogenic conditions at source-zone groundwater contaminated with a biodiesel blend (B20), *Biodegradation*, 2013, **24**(3), 333–341.

58 M. Sait, K. E. Davis and P. H. Janssen, Effect of pH on isolation and distribution of members of subdivision 1 of the phylum Acidobacteria occurring in soil, *Appl. Environ. Microbiol.*, 2006, **72**(3), 1852–1857.

59 A. M. Maszenan, J. H. Tay, P. Schumann, H. L. Jiang and S. T. Tay, Quadrisphaera granulorum gen. nov., sp. nov., a Gram-positive polyphosphate-accumulating coccus in tetrads or aggregates isolated from aerobic granules, *Int. J. Syst. Evol. Microbiol.*, 2005, **55**, 1771–1777.